# Computation of the Density-Density Response Function in a Hofstadter Model

by Timo Zacharias, supervised by Michael Knap and Fabian Pichler

Technische Universität München

## Abstract

The Fractional Quantum Hall (FQH) effect in lattice systems provides a rich platform to study strongly correlated topological phases beyond the continuum limit. In this work, we investigate the FQH states at filling factors $\nu = 1/3$ and $\nu = 2/3$ within a Hofstadter model using a parton-based framework. Employing the Random Phase Approximation (RPA), we compute the density–density response function and use the Padé approximation to obtain its real-frequency behavior. The resulting excitation spectrum exhibits a gapped collective mode with characteristic magnetoroton modes appearing on top of a continuum of excitations. Moreover, we can identify distinct regions in the spectrum that originate from excitations involving different numbers of partons.

## Parton Model

The FQHE was discovered in 2D electron liquids (area A) with a strong perpendicular magnetic field $B$. The electrons fill up Landau levels (LL's), to an amount given by $\nu_e$ [Tong 2016].

**Idea of the parton model:** Explain the FQHE at fractional $\nu_e$ by decomposing the electrons into $M$ partons (charge $q_i$) of species $i = 1, \ldots, M$, that exhibit an integer QHE, i. e. $\nu_i$ integer [Jain 1989].

- On operator level in **real space**: $\hat{\boldsymbol{\Psi}}_e(\vec{x}, \tau) = \hat{\boldsymbol{\Psi}}_1(\vec{x}, \tau) \cdot \ldots \cdot \hat{\boldsymbol{\Psi}}_M(\vec{x}, \tau)$ („Parton factorization")
- Constraint $\mathbf{1} \equiv q_e = q_1 + \ldots + q_M$
- For all partons we have $\frac{N}{\nu_i} = \frac{A \cdot B}{\phi} = \frac{A \cdot B \cdot q_i e}{2\pi\hbar} \quad \Rightarrow \quad q_i = \frac{\nu_e}{\nu_i}$ and $\nu_e = (\sum_i^M \nu_i)^{-1}$
- For $\boldsymbol{\nu = 1/3}$: $\boldsymbol{M = 3}$ parton species, $q_i = \frac{1}{3}$ and $\nu_i = 1$ for **all i = 1, 2, 3**;
- For $\boldsymbol{\nu = 2/3}$: $\boldsymbol{M = 3}$ parton species, $q_1 = -\frac{1}{3}$, $\nu_1 = -2$ and $q_i = \frac{2}{3}$, $\nu_i = 1$ for **= 2, 3**.

### Transition to Lattice Models and my Model

- In a lattice model, we do not have LL's but only electron bands.
- For topologically non-trivial materials: connection between the filling factor $\nu$ in LL's and the sum of the Chern numbers of filled bands in a lattice model (by the TKNN formula) [Tong 2016].
- For the case of $\nu = 1/3$ and $\nu = 2/3$ we use a Hofstadter model to get the appropriate Chern numbers, they are schematically shown in the figures 1 and 2.

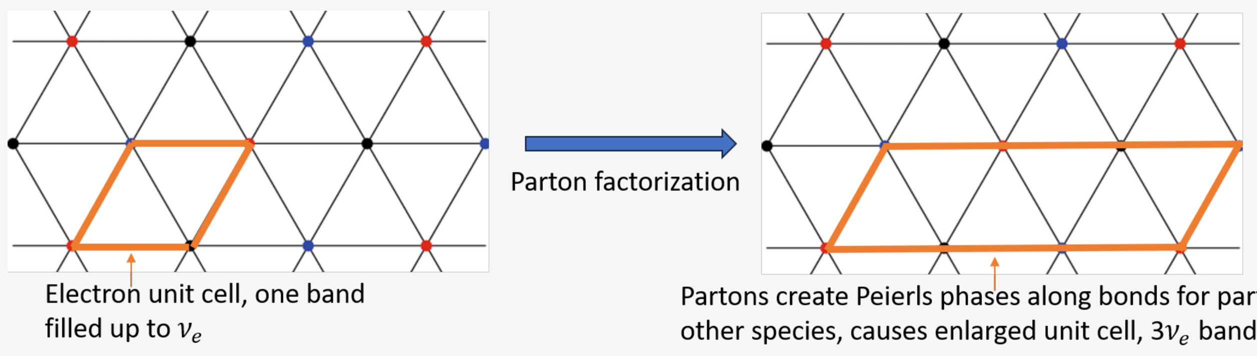


Figure 1. Triangular lattice used to model the parton models for both states, $\nu = 1/3$ and $\nu = 2/3$.

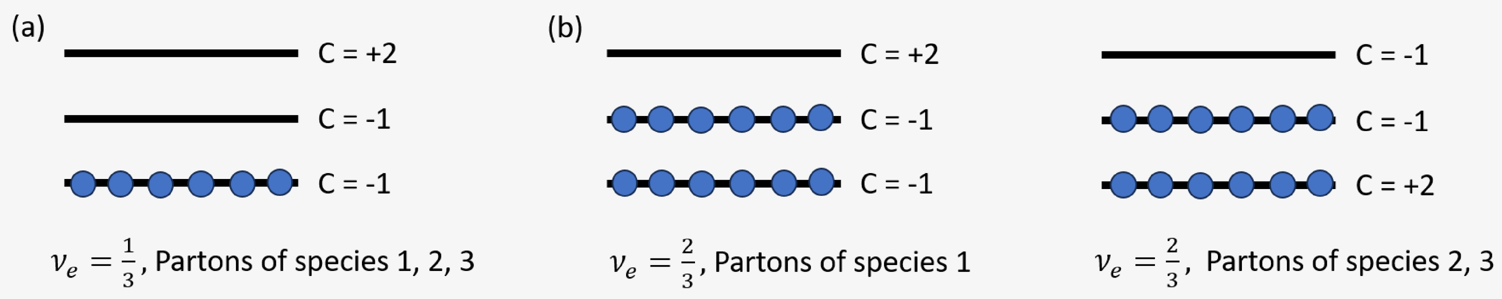


Figure 2. (a)For $\nu = 1/3$ we have three parton species, all of them have a charge $q_i = -1/3$ and a filling $\sum_\alpha C_\alpha = -1$. (b) For $\nu = 2/3$ there are three parton species, one of them with charge $q_1 = -1/3$ and $\sum_\alpha C_\alpha = -2$ (left) and two of them with $q_{2,3} = 2/3$ and $\sum_\alpha C_\alpha = +1$ (right).

## Neutral Excitations in a FQH state: Investigation via the Density-Density Response function

- FQH states are gapped $\Rightarrow$ particle-hole excitation spectrum is gapped.
- On top of this continuum there are collective excitation modes (**magnetoroton modes**) [Chengzhang 2012; Girvin et al. 1986].
- We want to investigate these neutral excitations for our lattice model of the $\nu = 1/3$ and $\nu = 2/3$ states by computing the Density-Density Response function, see eq. (1).

$$\chi(\vec{k}, \omega) = -\frac{i}{\hbar}\int_0^\infty e^{i(\omega + i\eta)t}\theta(t)\langle\left[\hat{\rho}_{\vec{k}}(t), \hat{\rho}_{-\vec{k}}(0)\right]\rangle. \tag{1}$$

- Diagrammatically, $\chi(\vec{k}, \omega)$ can be written as depicted in fig. 3
- employ the Random-Phase approximation, illustrated in fig. 3 to sum up all perturbation orders.

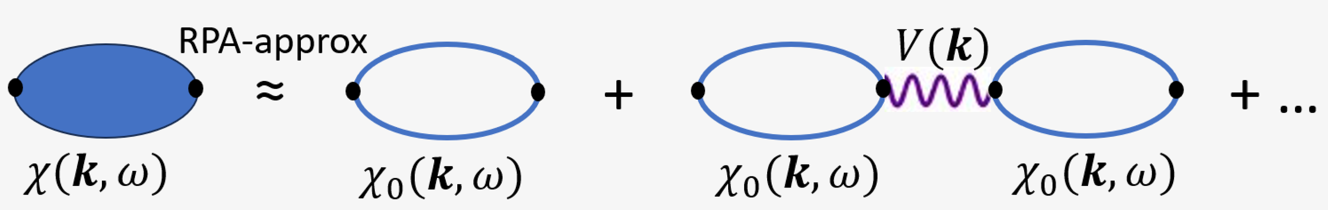


Figure 3. Diagrammatic representation of the density-density response function in the random phase approximation

- Summing up all terms in the RPA yields the following expression for $\chi(\vec{k}, \omega)$,

$$\chi(\vec{k}, \omega) = \frac{\chi_0(\vec{k}, \omega)}{1 - V(k)\chi_0(\vec{k}, \omega)}. \tag{2}$$

- To compute $\chi(\vec{k}, \omega)$ with the RPA we need to calculate $\chi_0(\vec{k}, \omega)$. Employing the parton-factorization for $\nu = 1/3$ and $\nu = 2/3$ yields the following diagrammatic contributions:

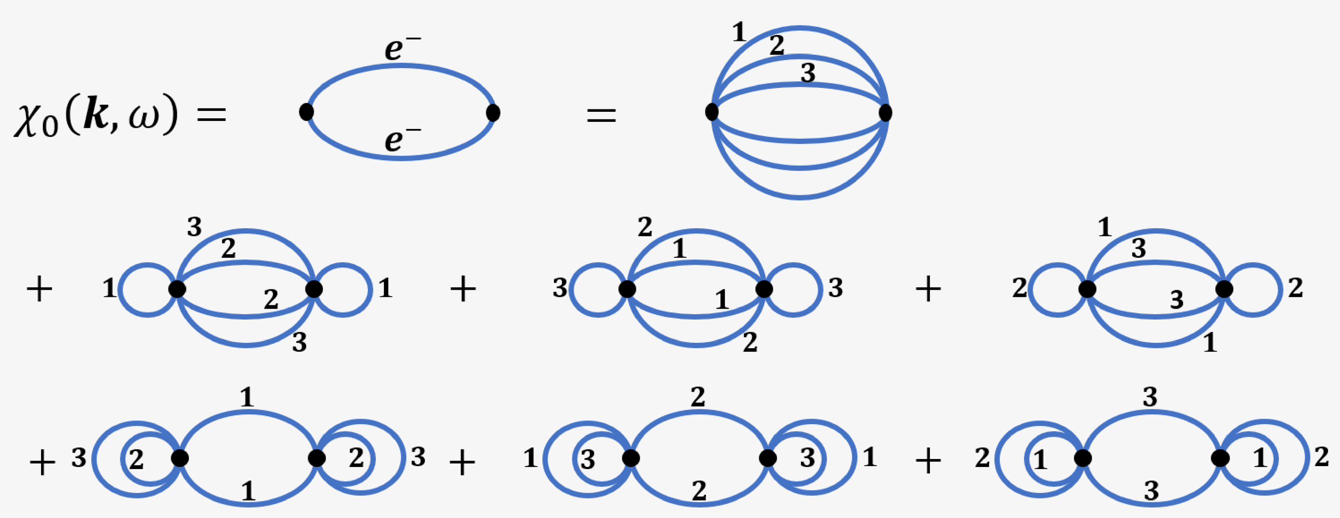


Figure 4. Diagrammatic Rerpresentation of $\chi_0(\vec{k}, \omega)$ after parton decomposition

## Problems with the Computation of $\chi(\vec{k}, \omega)$

- The diagrams depicted in figure 4 contain too many **convoluted sums** in momentum space $\Rightarrow$ cannot be computed exactly for realistic system sizes
- Solution so far: **Padê Approximation** [Beach et al. 2000], see fig. 5.

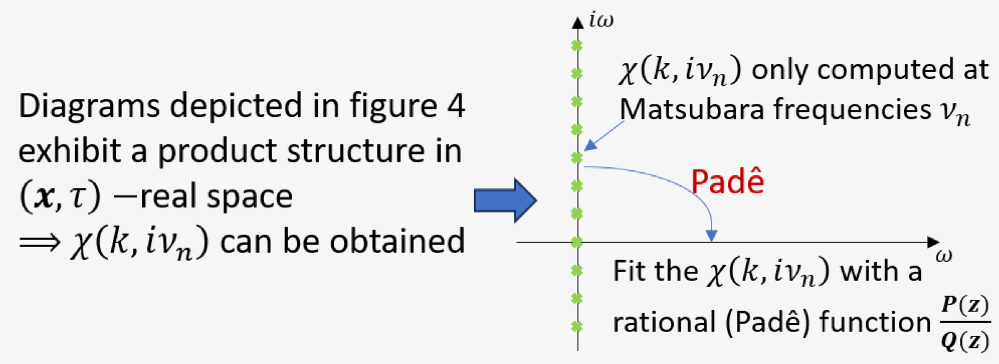


Figure 5. Illustration of the Padê Approximation procedure

## Results: Plots of $\mathcal{I}m(\chi(\vec{k}, \omega))$ along high-symmetry points $\Gamma M K \Gamma$

- We computed $\chi(\vec{k}, \omega)$ for the lattice model (figure 2) and assumed a **repulsive neirest-neighbor (NN) potential**.
- We applied the Padê approximation at different stages:
  **Variant A**: we apply Padê **after** doing the RPA, i. e. onto $\chi(\vec{k}, i\nu_n) \to \chi(\vec{k}, \omega)$, see figures 6 and 7.
  **Variant B**: we apply Padê **before** doing the RPA, i. e. by approximating the individual diagrams shown in fig. 4, and then doing RPA, see figures 8 and 9.

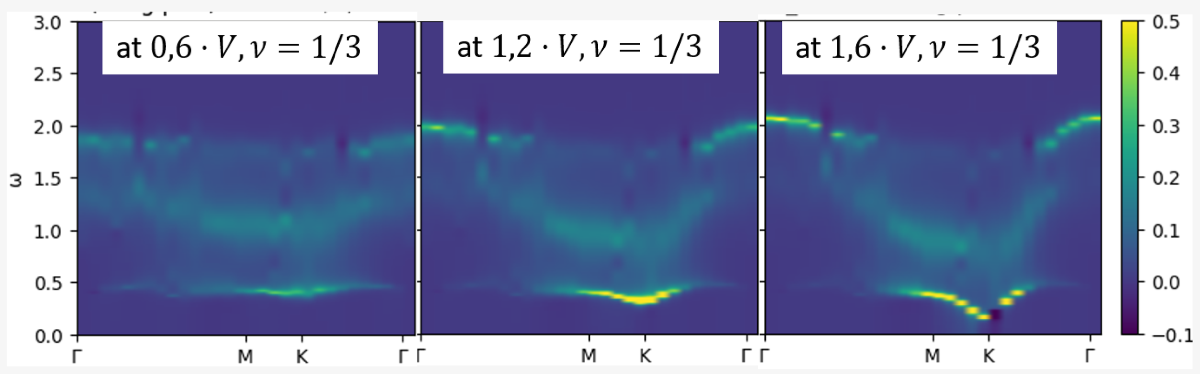


Figure 6. Variant A-$\mathcal{I}m(\chi(\vec{k}, \omega))$ at $\nu = 1/3$ and repulsive NN-potential V, with different strengths.

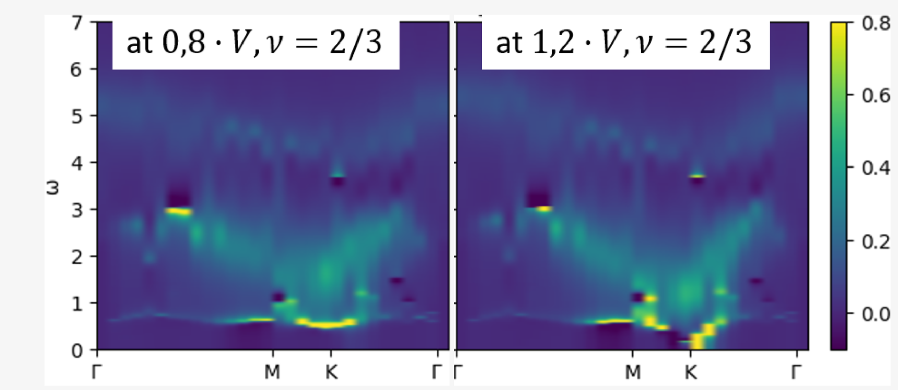


Figure 7. Variant A-$\mathcal{I}m(\chi(\vec{k}, \omega))$ at $\nu = 2/3$ and repulsive NN-potential V, with different strengths.

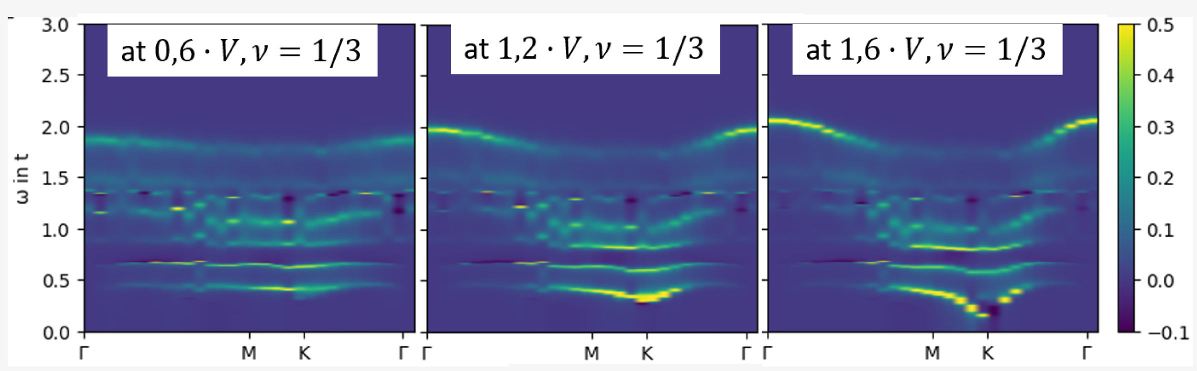


Figure 8. Variant B-$\mathcal{I}m(\chi(\vec{k}, \omega))$ at $\nu = 1/3$ and repulsive NN-potential V, with different strengths.

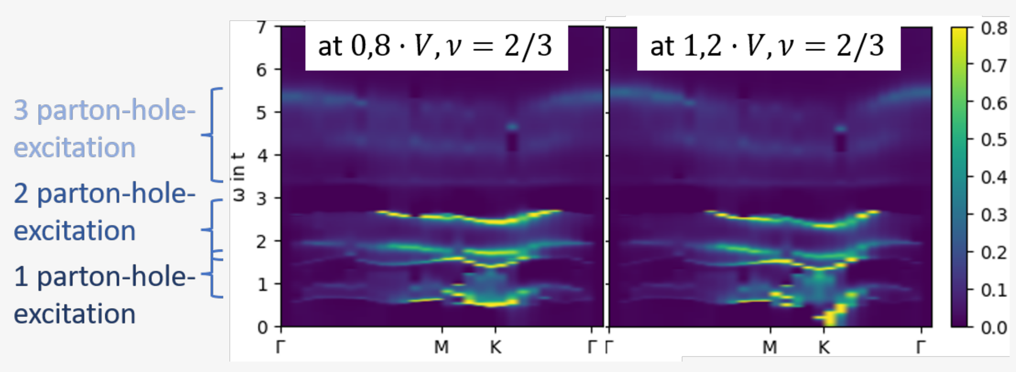


Figure 9. Variant B-$\mathcal{I}m(\chi(\vec{k}, \omega))$ at $\nu = 2/3$ and repulsive NN-potential V, with different strengths.

- For both variants, A and B, we observe a softening of the roton mode at the $K$-point, at equal interaction strengths $V$.
- Both variants, A and B, predict gapped spectra with a similar gap size.
- On the other hand, the fine structure differs, variant B seems to yield more sharp modes than the approximation scheme A.
- The different contributions to $\chi_0$, coming from the different diagrams in 4, can be identified, especially in variant B, see figure 9.
- To benchmark the right approximation method, we want to check the correctness of the presented results by exactly computing $\chi(\vec{k}, \omega)$, via (1), using Tensor Networks.

## References

- Tong, D. (2016). *Lectures on the Quantum Hall Effect*. arXiv: 1606.06687 [hep-th]. URL: https://arxiv.org/abs/1606.06687.
- Chengzhang, S. (Apr. 2012). "THE CHERN–SIMONS–LANDAU–GINZBURG THEORY OF THE FRACTIONAL QUANTUM HALL EFFECT". In: *International Journal of Modern Physics B* 06. DOI: 10.1142/S0217979292000037.
- Beach, K. S. D., R. J. Gooding, and F. Marsiglio (Feb. 2000). "Reliable Padé analytical continuation method based on a high-accuracy symbolic computation algorithm". In: *Physical Review B* 61.8, pp. 5147–5157. ISSN: 1095-3795. DOI: 10.1103/physrevb.61.5147. URL: http://dx.doi.org/10.1103/PhysRevB.61.5147.
- Jain, J. K. (Oct. 1989). "Incompressible quantum Hall states". In: *Phys. Rev. B* 40 (11), pp. 8079–8082. DOI: 10.1103/PhysRevB.40.8079. URL: https://link.aps.org/doi/10.1103/PhysRevB.40.8079.
- Girvin, S. M., A. H. MacDonald, and P. M. Platzman (Feb. 1986). "Magneto-roton theory of collective excitations in the fractional quantum Hall effect". In: *Phys. Rev. B* 33 (4), pp. 2481–2494. DOI: 10.1103/PhysRevB.33.2481. URL: https://link.aps.org/doi/10.1103/PhysRevB.33.2481.